2005

Optical Cavity Design of Integrated MicroPhotonic Wideband Adaptive RF Signal Processor

Rong Zheng
Edith Cowan University

Zhenglin Wang
Edith Cowan University

Kamal Alameh
Edith Cowan University

Optical Cavity Design of Integrated MicroPhotonic wideband adaptive RF Signal Processor

Rong Zheng, Zhenglin Wang and Kamal E. Alameh

Centre for MicroPhotonic Systems,
Electron Science Research Institute, Edith Cowan University,
Joondalup, WA, 6027, Australia.
Tel. +61-8-6304 5732, Fax +61-8-6304 5302, Email: r.zheng@ecu.edu.au

ABSTRACT

In this paper, we analyse the beam propagation within the optical cavities of an integrated MicroPhotonic adaptive RF signal processor, and optimize the optical beam diameter.and incidence angle that maximize the number of taps to realize high-resolution RF processor. Simulation results show that for a 1mm-diameter collimated Gaussian beam, 16 taps per cavity can be achieved for a 20mm-long cavity, and that there is no need for a diffractive optical element (DOE) to re-collimate the Gaussian beam within the cavity. The tolerance of the MicroPhotonic processor to changes in optical cavity length, which degrade the beam overlapping with the active areas of the photodetector elements, is also quantitatively analysed.

Keywords: Optical substrate, RF signal processing.

1. INTRODUCTION

Owing to the ultra-high bandwidth available in optical media, photonic adaptive RF signal processing has inherent advantages over all-electronics signal processing. A number of studies have been demonstrated in developing adaptive photonic RF signal processors [1,2], including fibre optical cavities based true-time delay generation for the realization of transversal RF filters [3, 4]. The use of multiple wavelength sources of variable power levels and separations has also been proposed [5]. However, the capabilities of these filter structures are limited by two fundamental issues, namely, (i) the substantial phase-induced intensity noise caused by long coherence length of the laser source, and (ii) the complexity of reconfiguring them to realize arbitrary transfer characteristics. To overcome these limitations, an 8×8 true-time delay module that integrates holographic-grating couplers and graded index (GRIN) lenses on top of optical substrates has been proposed for a K-band phased array antenna beamforming [6]. In their module, a portion of the substrate guided wave is extracted out each time the wave encounters the output holographic-grating coupler and focused back into optical fibres. However, coupling the optically delayed signals into optical fibres limits the maximum number of delays that can be synthesized.

Recently, we have proposed a new Microphotonic transversal RF signal processor [7, 8] in which a VCSEL array, a 2D ultra-wideband photoreceiver array and a multi-cavity optical substrate are integrated to achieve an arbitrary high-resolution RF filter transfer characteristics with no optical interference. This is based on using optical cavities of different lengths to generate a number of delayed RF-modulated optical signals whose amplitudes are independently adjusted by varying the gain profile of the photo-receiver array to realise adaptive RF signal processing. The unique feature of our proposed approach is that all the true-time-delay optical substrate, optical source and receiver will be integrated into one single substrate. As a result, it significantly reduces the device size while eliminating the most difficult packaging problem associated with the delicate interfaces between optical fibers and optical substrate. Such a monolithic approach offers great precision for the RF phase control than the fiber delay-lines due to the sub-micrometer accuracy of optical substrate. Also, the gain for each photodetector array can be individually set, making this structure more agile and robust.

In this paper, we extend the analysis of the Microphotonic transversal RF signal processor by investigating the optical beam propagation within the cavities of the integrated MicroPhotonic adaptive RF signal processor, and evaluating the maximum number of taps that can be generated by each cavity. Also, the tolerance of the lateral displacement of the last beam on the photodetector in terms of the incidence angle deviations, the flatness and the parallelism of the cavity are discussed. Results show that for a cavity length of 20mm and a 1.0mm-diameter optical beam incident at an angle of 2.86°, there is no need to use a diffractive optical element to re-collimate the expanding beam, and that up to 16 RF delayed signals per cavity can be generated. Tolerance analyses show that in order to photodetect the optical beams, the lateral beam displacement must be less than 200μm. Also, the incidence angle must be aligned within ±28", the cavity flatness must be within ±100 μm and the parallelism between the coated surfaces of the cavity must not exceed ±15".

2. STRUCTURE OF THE INTEGRATED MICROPHOTONIC ADAPTIVE RF SIGNAL PROCESSOR

Figure 1 shows the schematic diagram of our proposed integrated MicroPhotonic adaptive RF signal processor. The input RF signal is firstly amplified by a low-noise amplifier (LNA) and then split equally into N RF signals which modulate the N elements of the $1\times N$ 850nm VCSEL array. Each RF-modulated optical beam

generated by a VCSEL element must be firstly collimated and through a diffractive optical component (DOE) diffracted with an angle to launch into the optical substrate.

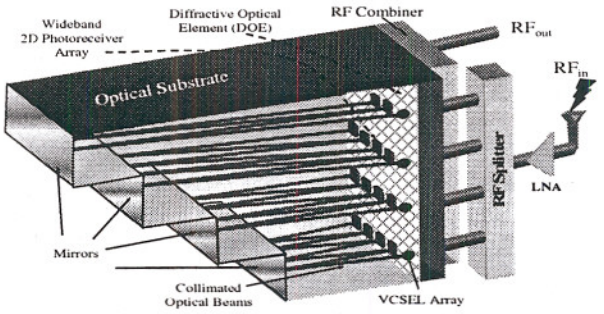

Figure 1. Architecture of integrated MicroPhotonic adaptive RF signal processor.

Figure 2 shows the detailed interface between the VECSEL/Photodetector chip and the optical substrate. To generate M delayed RF modulated optical signals, one side of the optical substrate is mirror coated while the other side is high-reflection (HR) coated (~90%) so that an optical beam entering the optical substrate at an incidence angle θ propagates within the cavity in a zigzag mode. Every time a beam bounces off the HR coated surface of the cavity a small fraction of the beam's power is transmitted out of the cavity and focused, through a microlens, on the photodetector array. Therefore a number of delayed RF-modulated optical signals is generated and detected by a photoreceiver array.

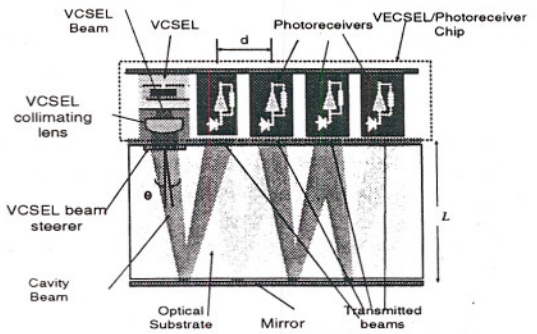

Figure 2 The schematic interface between the VECSEL/Photodetector chip.

For a given cavity length, L, optical substrate refractive index n, and photodetector element spacing d, the sampling time is given by:

$$\tau_s = \frac{n\sqrt{4L^2 + d^2}}{c} \qquad (2.1)$$

To attain an adequate SNR (signal to noise ratio) and maintain the crosstalk between the adjacent channels less than -30dB, the minimum photodetector element spacing must satisfy the following equation:

$$d > 4\omega \qquad (2.2)$$

where ω is the incident beam waist. Thus, the minimum incident angle θ is given by:

$$\theta = \arctan(d / 2L) \qquad (2.3)$$

For an RF signal processor operating over a 5GHz bandwidth, the cavity length must not exceed 20mm, which corresponds to a sampling frequency of 10GHz. For an incident optical beam diameter of 1mm, the minimum incident angle θ is about 2.86°.

3. Optical Cavity Design of the Integrated MicroPhotonic Adaptive RF Signal Processor

3.1. Optical beam collimation

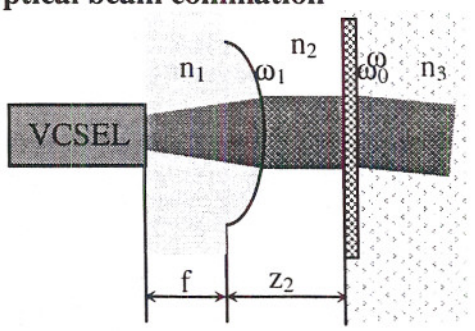

Figure 3. Schematic diagram of the VCSEL collimator.

Without collimation, the output Gaussian beam from a VCSEL element diverges very quickly in free space. Therefore, before it is launched into the optical cavity, it must be collimated. Figure 3 shows the evolution of the VCSEL beam as it propagates through a collimator and a steering diffractive optical element. Assume that the waist of the VCSEL located at the focus point of a lens is ω_0. To avoid beam truncation that is due to the limited aperture size of the lens [9], the diameter of the collimating lens must be at least twice the size of collimated beam radius, ω_1. The output optical beam diameter is given by :

$$\omega_1^2(x) = \omega_0^2\left[1 + \left(\frac{\lambda f}{\pi \cdot n_1 \cdot \omega_0^2}\right)^2\right] \qquad (3.1)$$

where n_1 is the refractive index of collimator lens. Similarly, the beam waist at the surface of the DOE is given by:

$$\omega_2^2(x) = \omega^2\left[1 + \left(\frac{\lambda z}{\pi \cdot n_1 \cdot \omega^2}\right)^2\right] \qquad (3.2)$$

where z is the spacing between the collimator and the optical cavity.

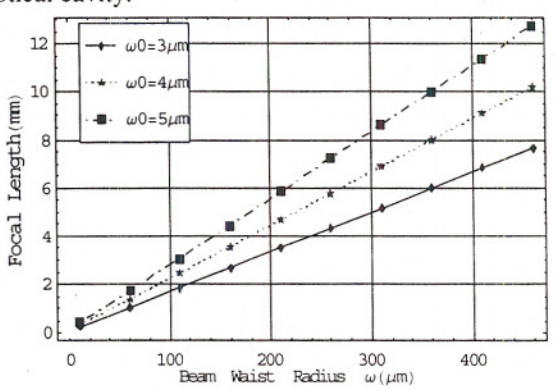

Figure 4. Required focal length versus the beam-waist radius ω for different VCSEL input beam sizes.

Figure 4 shows the focal length of the collimator lens as a function of the output beam waist radius ω_2 with various VCSEL input beam waist ω_0. In our calculation, we assume that λ=850nm, n_1= 1.5, n_2=1, and z =50μm. It is shown that the required focal length of the collimating lens increases linearly with the incident beam size ω.

3.2. The maximum number of generated RF sampling signals.

Since the incident beam is launched into the optical cavity with an angle θ, the beam expands after it is reflected off the cavity surfaces several times. Generally, the expanding beams overlap at the photodetector array, thus limiting the maximum number of generated RF sampling signals. To generate N delayed RF signals per cavity, the optical beam propagation in the cavity must reflect N times off the mirror-coated side with minimum overlapping between adjacent beams. Therefore, the total propagation length of optical beam in the cavity must be within the Rayleigh range of the incident beam, which is given by

$$Z_N = \frac{2L \cdot N}{\cos\theta} < Z_R \qquad (3.4)$$

where $Z_R = \frac{\pi \cdot n_3 \cdot \omega_0^{\,2}}{\lambda}$ and n_3 is the refractive index of the glass substrate. For BK7 glass substrate, n_3 = 1.52.

Figure 5 shows the maximum number of delayed RF signals with negligible beam overlapping versus the incident beam waist. Negligible beam overlapping results in more than -50 dB crosstalk, which corresponds to a beam spacing of 4ω, where ω is the beam waist. It is shown that when the incident beam waist increases the cavity can tolerate more delayed RF signals. For example, when the incident beam size is 1mm, up to 34 sampling beams can be generated within the cavity.

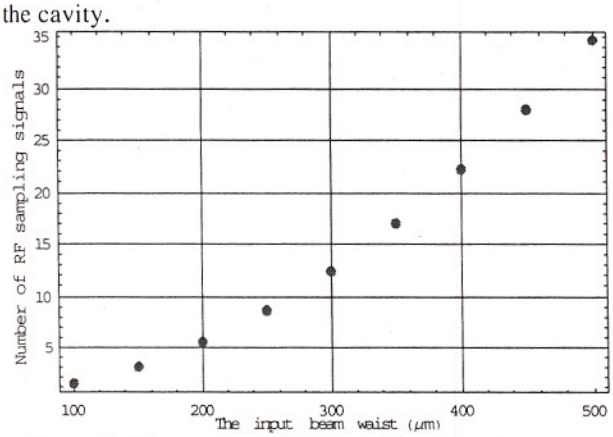

Figure 5. The number of RF sampling signals versus input beam size.

The above simulation results are obtained, assuming that all delayed RF-modulated beams are detected within the Rayleigh distance, and hence the optical beam does not need to be re-collimated as it propagates within the cavity. If more delayed RF-modulated beams are needed, a DOE film must be integrated between the photoreceiver chip and the optical substrate to appropriately focus the diverging beam and maintain its diameter within an acceptable range. Note, however, that if the spacing between the detected beams is reduced to 3ω, the crosstalk between the beams will increase to -30 dB and for a photoreceiver array size of 24x24mm, the MicroPhotonic processor can accommodate 16 optical cavities, each generating 16 taps, thus realising 256 taps without employing a DOE film. This makes the processor more robust and cost-effective.

3.3. Receiving Lens array.

Broadband RF photodetectors must have a small active area (hence a small capacitance) in order to maximise their bandwidth. For example, a typical 5 GHz photodetector has an active area of around 60μm. Therefore, the optical beams must be focused in order to be detected by the photoreceiver array with minimum loss. In our design, we assume that the pitch of photoreceiver array is the same as the spacing of the Delayed RF-modulated optical beams and its detector diameter is 60 μm. A lens array is used to focus the individual beam to the photodetector array.

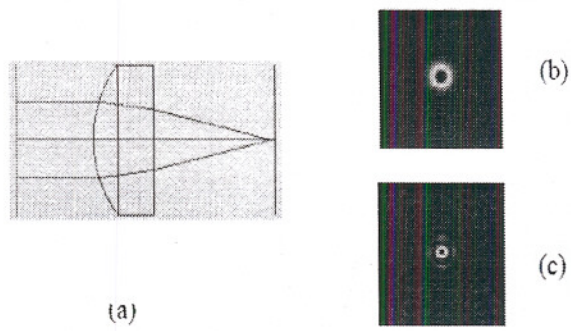

Figure 6. Beam propagation through the focusing microlens and beam spot at the photodetector for different microlens diameters
(a) The schematic diagram of the receiving microlens.
(b) Beam spot at the photodetector, input beam diameter is 1mm
(c)Beam spot at the photodetector, input beam diameter is 2mm

Figure 6 shows the focusing microlens configuration and the focused beam at the focal plane where the photodetector is placed. In this simulation, which was run using ZEMAX, a graded-index microlens of focal length 1.9mm and diameter of 2mm is used. Figure 6(b) shows the beam spot at the photodetector when the photodetector aperture diameter is twice the beam diameter. It is obvious that in this case the beam can be focused and detected by the photodetector with minimum loss. Figure 6 (c), shows the beam spot at the photodetector when the photodetector aperture diameter is equal to the beam diameter. In this case, the optical beam diffracted of the lens edge and less optical power is photodetected, resulting in higher loss.

4. Tolerance Considerations

The proposed integrated MicroPhotonic RF signal processor generates a large number of delayed RF signals which are detected by the photoreceiver array. The output optical beam needs to be focused at the

photodetector array precisely.. Since the maximum lateral displacement of all optical beams is limited, a special attention must be devoted to the tolerance of the optical substrate design to ensure that the crosstalk and SNR performances are adequate. In particular, the impact of the incident beam angle and lateral beam displacement must be examined using extensive ray-tracing simulation.

Figure 7 shows maximum allowable change in incidence angle, within which all optical beams propagating in the cavity are focused on the active are of the corresponding photodetector elements, versus the incidence angle. The simulation is carried out for the worse case lateral displacement where the beam has been reflected 16 times in the optical cavity. It is obvious that for a given lateral displacement, the tolerance to changes in incidence angle becomes more limited as the incidence angle increases. Therefore, designing the optical cavities to operate with a smaller launching beam angle is always a better option. For example, for an incidence angle of 2.86°, the maximum allowable error in incidence beam angle is around 28", which is achievable with the current technology.

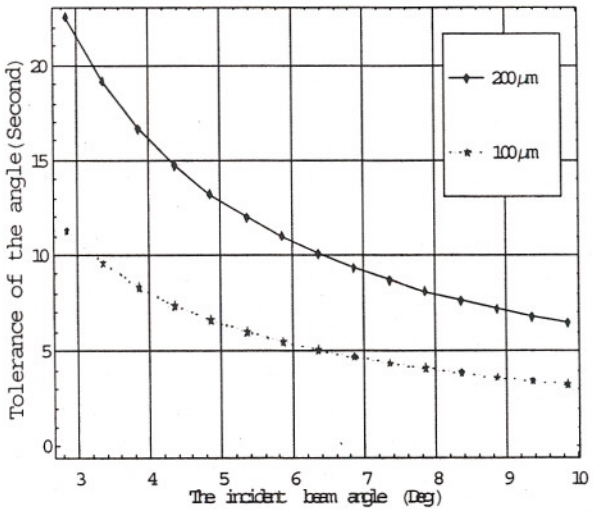

Figure 7. The tolerance to changes in incidence beam angle for different lateral displacements.

The lateral displacement of the 16th beam versus the cavity flatness for different beam incidence angles is shown in Figure 8. It is obvious that by reducing the incident beam angle, a better tolerance to change in cavity flatness is achieved. To limit the lateral displacement within ±200 μm, the cavity flatness must be within a range of ±100 μm.

Figure 9 shows the simulation results of the 16th sampling beam lateral displacement versus the cavity substrate parallelism. To keep the lateral displacement of the beam within ±200 μm, the parallelism of the optical substrates should be in the range of ±15 arc seconds. This manufacture precision is readily available for surface areas larger than 10cm×10cm.

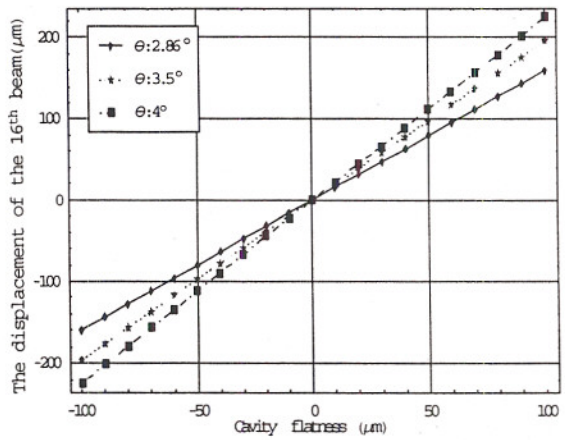

Figure 8. The lateral displacement of the 16th beam versus the cavity flatness.

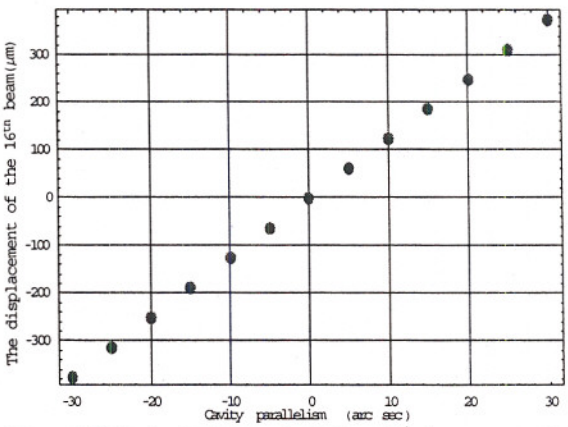

Figure 9.Lateral displacement of the 16th beam versus cavity parallelism.

5. CONCLUSIONS

In the paper, we have designed the optical cavity for an integrated MicroPhotonic RF signal processor with the aim to generate 16 taps per cavity. Analyses have shown that for an optical cavity length of 20mm and a 1-mm beam incident at 2.86°, 16 delayed RF signals can be generated within the cavity without the need to use a diffractive optical element to collimate the expanding beam within the cavity. Tolerance analyses have shown that the lateral displacement of the beam at the last photodetector element must be less than 200μm in order to detect the optical beam at the photodetector with minimum loss. The incident beam angle must also be aligned within 28". In addition, a cavity flatness of ±100 μm and a cavity parallelism of ± 15" are needed to maintain an adequate crosstalk performance.

6. ACKNOWLEDGEMENT

This work was supported by the Office of Science and Innovation, Western Australian Government.

7. REFERENCES

[1] F. Ramos J. Marti, V. Polo and D. Moodie. " Photonic tunable microwave filters employing electroabsorption modulators and wideband chirped fibre gratings". Electronics Letters, IEE, 35(4):305-306, 1999.

[2] D. Pastor, J. Capmany, S. Sales, P. Munoz, and B. Ortega, "Reconfigurable fiber-optic-based RF filters using current injection in multimode lasers," Photonics Technology Letters, IEEE, vol. 13, no. 11, pp. 1224– 1226, 2001

[3] K.E. Alameh, E.H.W. Chan, and R.A. Minasian. "High skirt selectivity photonics based bandpass filters". In International Topical Meeting on Microwave Photonics MWP'01, pages 191{194, USA, 2002.

[4] D. B. Hunter and R. A. Minasian. "Photonic signal processing of microwave signals using an active-fibre bragg-grating-pair structure". Microwave Theory and Techniques, IEEE Transactions on, 45(8):1463-1466, 1997.

[5] R. A. Minasian and K.E. Alameh. "Photonic signal processing". In 27th triennial General Assembly of the International Union of Radio Science, page 192, The Netherlands, 2002.

[6] Yihong Chen and Ray T. Chen. "A fully packaged true time delay module for a k-band phased array antenna system demonstration". *IEEE Photon. Technol. Lett.*, 14(8):?, 2002.

[7] K. Alameh, A. Bouzerdoum, R. Zheng, S. Ahderom, M. Raisi, K. Eshraghian, X.Zhao, Z. Wang. "MicroPhotonic Interference Mitigation Filter for Radio Telescope", SPIE International Symposium Microelectronics, MEMS, and Nanotechnology. 10- 12 Dec. 2003, Peth, WA. Australia.

[8] R.Zheng, K.E.Alameh, Z.Wang, "A Microphotonic Transversal RF Signal Processor with no Laser Coherence Noise", Microwave and Optical Technology Letters, 2005 , to be published.

[9] http://wwww.mellesgriot.com/products/optics/gb_2_3.htm